# Joint Experimental and Theoretical Studies of the Mechanism for the Gas Phase Elimination Kinetics of Methyl 2,2-Dimethyl-3-hydroxypropionate

**Alexandra Rotinov,[†] Beatriz Ramirez,[‡] Luz Escalante,[‡] Desiree Pereira,[‡] Tania Córdova,[‡] and Gabriel Chuchani*[,†]**

*Centro de Química, Instituto Venezolano de Investigaciones Científicas (IVIC), Apartado 21827, Caracas, Escuela de Química, Facultad de Ciencias, Universidad Central de Venezuela, Apartado 1020-A, Caracas, Venezuela*

*Received: December 2, 2008; Revised Manuscript Received: February 26, 2009*

Methyl 2,2-dimethyl-3-hydroxypropionate was found to decompose, in a static system, mainly to methyl isobutyrate and formaldehyde. The reaction rates were affected in packed and unpacked clean Pyrex vessels, demonstrating little but significant surface effect. However, in vessels seasoned with allyl bromide this reaction was homogeneous and unimolecular and followed a first-order law. The working temperature range was 349−410 °C and the pressure range was 64−162 Torr. The variation of the rate coefficient with temperature is expressed by the following Arrhenius expression: log $k_1$ ($s^{-1}$) = [(11.43 ± 0.57) − (180.4 ± 7.2) kJ $mol^{-1}$] × $(2.303RT)^{-1}$. Methyl 2,2-dimethyl-3-hydroxypropionate was found to be 1.4 times greater in the rate of elimination than methyl 3-hydroxypropionate. Apparently, steric acceleration may be considered responsible in the process of decomposition. The theoretical calculation of the kinetics and thermodynamics parameters, at the B3LYP/6-211G** level of theory, are in reasonably good agreement with the experimental values obtained. These calculations imply a molecular mechanism involving a concerted nonsynchronous transition state where abstraction of the hydroxyl hydrogen by the oxygen of the carbonyl ester is a determining factor and the transition state is late in the reaction coordinate.

## I. Introduction

Yates et al. reported the thermal decomposition of β-hydroxy ethyl esters in xylene solution[1] and in evacuated sealed gas tubes.[2] The reactions were found to be homogeneous and monomolecular with negative entropies of activation in the range of −8.7 to −12.6 eu. According to these results of typical unimolecular reactions involving a cyclic transition state, it was proposed that β-hydroxy ethyl esters pyrolyzed through a six-membered cyclic transition state to give mixtures of esters and aldehydes or ketones [reaction 1 step **1**]. However, the presence of at least a $C_\beta$−H bond at the

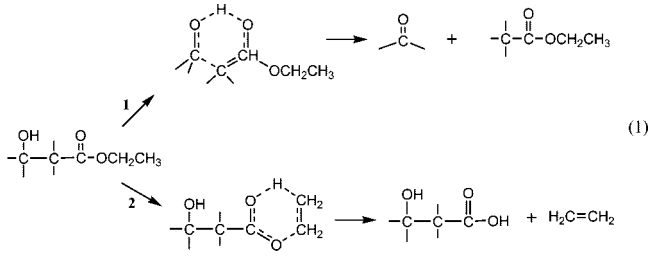


(1)

alkyl side of the ester like the ethyl group in the β-hydroxy esters, $R^1R^2C(OH)CH_2COOCH_2CH_3$, may lead to a competing parallel reaction with decomposition at the alkyl side of the esters[3,4] as shown in reaction1 step **2**.

When the ethyl group, $CH_3CH_2$, is replaced by the methyl group, $CH_3$, in β-hydroxy esters, the thermal elimination proceeds in a single process similar to that described in reaction1, step **1**. In this respect, Taylor et al.[5] reported the gas phase pyrolysis kinetics of primary, secondary, and tertiary methyl β-hydroxy esters producing the methyl ester and the corresponding carbonyl compound. The comparative rate coefficients were found to increase from primary to the tertiary hydroxy ester.

A MNDO molecular orbital theory was employed to investigate the pyrolysis mechanism of methyl β-hydroxypropionate[6] where a pseudocyclic six-membered transition state was considered. The results were believed, due to inherent shortcomings, to be at least qualitatively correct.

Theoretical studies on the gas phase of three methyl β-hydroxy esters: the primary methyl 3-hydroxypropanoate, secondary methyl 3-hydroxybutanoate, and tertiary methyl 3-hydroxy-3-methylbutanoate were carried out at the MP2/6-21G(d) and MP2/6-211+G(d,p) levels of theory.[7] The authors claimed that the calculated kinetic parameters agreed well with the experimental results. Their conclusion is rather surprising because the calculated energies of activation gave differences of more than 24 kJ/mol when compared to the experimental result. In addition to this fact, the calculated log $A$ is about 2 units greater than the experimental value. The estimated value of log $A$ = 13.2 is the preferred experimental value for a four-membered cyclic transition state type of mechanism[8] rather than the six-membered cyclic transition state which takes place with the β-hydroxy esters decomposition.

Years later, several methyl β-hydroxy esters were thermally decomposed in *m*-xylene solutions.[9] The reactions were found to be homogeneous and unimolecular and to follow a first-order law. The products formed are methyl acetate and the corresponding aldehyde or ketone. The rate of decomposition in the gas phase[5] was found to be greater than in *m*-xylene solutions,[9] and the experimental data suggested a semipolar six-membered cyclic transition state as postulated for other β-hydroxy compounds.

* Corresponding author. E-mail: chuchani@ivic.ve.
† IVIC.
‡ Universidad Central de Venezuela.

10.1021/jp810649w CCC: $40.75 
Published on Web 03/23/2009

**SCHEME 1**

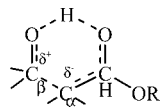

An interesting fact in the mechanistic interpretation of these elimination kinetics of $\beta$-hydroxy esters is that if $C_\beta-C\alpha$ bond polarization, in the sense $C_\beta^{\delta+}\cdots C_\alpha^{\delta-}$, is rate determining (Scheme 1), the presence of an electron releasing group, such as an alkyl group, at the $C_\alpha$ should decrease the rate of decomposition. Yet, the work of Yates et al.[2] showed that the rate for ethyl 3-hydroxy-2-methylbutanoate is about 3 times greater than that for ethyl-3-hydroxybutanoate.

Moreover, the thermal retroaldol reactions of several substituted $\beta$-hydroxy esters[10] in diglyme [bis(2-methoxyethyl)ether] at 170 °C where two methyl groups are substituted at the $C_\alpha$ of the $\beta$-hydroxy esters, that is, $ArCH(OH)C(CH_3)_2COOCH_3$, was found to be 20 times greater in rate than $ArCH(OH)CH_2COOCH_3$. The authors concluded that steric acceleration may be responsible in the process of decomposition and from theoretical examination steric strain release is the predominant controlling factor in the retroaldol reaction.

In view of the considerations that alkyl substituents at the $C_\alpha$ of the $\beta$-hydroxy esters seem to increase the rate of elimination with respect to the corresponding unsusbtituted compounds, the present work thought it of interest to examine the homogeneous elimination kinetics of a substrate containing two alkyl groups, such as the methyl groups at the $C_\alpha$, that is, methyl 2,2-dimethyl-3-hydroxypropionate, and compare it to the reference compound methyl 3-hydroxypropionate,[5] both under true gas phase conditions. An additional purpose of this work is to carry out a theoretical study at several computational levels for additional understanding about the mechanism of 2,2-dimethyl-3-hydroxypropionate and to compare the kinetics and thermodynamics parameters with the experimental values.

## II. Computational Method and Model

The reaction path for the gas phase decomposition reaction of 2,2-dimethyl-3-hydroxypropionate into methyl isobutyrate and formaldehyde was studied using electronic structure calculations at MP2/6-21G, B3LYP/6-21G*, B3LYP/6-21G**, B3LYP/6-211G**, and PBEPBE/6-211G** levels of theory as implemented in Gaussian 03W.[11] The Berny analytical gradient optimization routines were used. The requested convergence on the density matrix was $10^{-9}$ atomic units, the threshold value for maximum displacement was 0.0018 Å, and that for the maximum fore was 0.00045 hartree/Bohr. The transition states search was performed using Quadratic Synchronous Transit protocol as implemented in Gaussian 03W. The nature of stationary points was established by calculating and diagonalizing the Hessian matrix (force constant matrix). TS structures were characterized by means of normal-mode analysis. The unique imaginary frequency associated with the transition vector (TV), i.e., the eigenvector associated with the unique negative eigenvalue of the force constant matrix, has been obtained. Intrinsic reaction coordinate (IRC) calculations were performed to verify that the transition state structures connect the reactant and products in the reaction path.

Thermodynamic quantities such as zero point vibrational energy (ZPVE), temperature corrections ($E(T)$), and absolute entropies ($S(T)$), were obtained from frequency calculations and consequently, the rate coefficient can be estimated assuming that the transmission coefficient is equal to 1. Temperature corrections and absolute entropies were obtained assuming ideal gas behavior from the harmonic frequencies and moments of inertia by standard methods[12] at average temperature and pressure values within the experimental range. Scaling factors for frequencies and zero point energies for MP2 and B3LYP methods used are taken from the literature, in the case of PBEPBE method the B3LYP value was used.[13]

The first-order rate coefficient $k(T)$ was calculated using the TST[14] and assuming that the transmission coefficient is equal to 1, as expressed in the following expression:

$$k(T) = (KT/h)\exp(-\Delta G^{\#}/RT)$$

where $\Delta G^{\#}$ is the Gibbs free energy change between the reactant and the transition state and $K$ and $h$ are the Boltzmann and Plank constants respectively.

$\Delta G^{\#}$ was calculated using the following relations:

$$\Delta G^{\#} = \Delta H^{\#} - T\Delta S^{\#}$$

and

$$\Delta H^{\#} = V^{\#} + \Delta\mathrm{ZPVE} + \Delta E(T)$$

where $V^{\#}$ is the potential energy barrier and $\Delta$ZPVE and $\Delta E(T)$ are the differences of ZPVE and temperature corrections between the TS and the reactant, respectively. Entropy values were calculated from vibrational analysis and using Chuchani–Cordova's idea of factor $C^{\mathrm{exp}}$.[15] This factor has the purpose of rationalizing the limitations of the theoretical methods because they do not consider the collisional entropy, only the analysis of a single molecule. In this respect, the theoretical estimations of $\Delta G^{\#\mathrm{theo}}$, $\Delta S^{\#\mathrm{theo}}$, and log $A$ are generally far off from the experimental values. Therefore,

$$\Delta H^{\#\mathrm{exp}} \cong \Delta H^{\#\mathrm{theo}} \text{ and, consequently, } E_a^{\mathrm{exp}} E_a^{\mathrm{theo}}$$

$$\text{we expect that } \Delta G^{\#\mathrm{exp}} \cong G^{\#\mathrm{theo}}$$

$$\text{therefore, } \Delta G^{\#\mathrm{exp}} - E_a^{\mathrm{exp}} = C^{\mathrm{exp}}, \text{ we obtain } \Delta G^{\#\mathrm{theo}} = E_a^{\mathrm{theo}} + C^{\mathrm{exp}}$$

where $E_a$ is the activation energy, and the superscripts exp and theo refer to experimental and theoretical values respectively and the parameter $C^{\mathrm{exp}}$ is

$$C^{\mathrm{exp}} = nRT - T\Delta S^{\#\mathrm{exp}}, n = 1 \text{ unimolecular reaction}$$

$C^{\mathrm{exp}}$ includes the contribution of colisional entropy which has not been considered in frequency calculations (isolated molecules). Using

$$\Delta G^{\#\mathrm{theo}} = \Delta H^{\#\mathrm{theo}} - T\Delta S^{\#\mathrm{theo}}$$

$\Delta S^{\#\mathrm{theo}}$ was obtained. From $\Delta S^{\#\ \mathrm{theo}}$, $\Delta G^{\ \#\mathrm{theo}}$, log $A$, and the rate coefficients can be calculated

## III. Results and Discussion

The gas phase elimination of methyl 2,2-dimethyl-3-hydroxypropionate at the temperature range 349 − 410 °C and pressure

**TABLE 1: Ratio of Final ($P_f$) to Initial Pressure ($P_0$) of Methyl 2,2-Dimethyl-3-hydroxypropionate**

| temp (°C) | $P_0$ (Torr) | $P_f$ (Torr) | $P_f/P_0$ | av |
|---|---|---|---|---|
| 369.2 | 96 | 186.5 | 1.94 | 2.06 |
| 380.5 | 106 | 215 | 2.03 | |
| 390.5 | 133 | 275 | 2.07 | |
| 399.1 | 112 | 226.5 | 2.02 | |
| 410.0 | 112 | 251.5 | 2.24 | |

range 64−162 Torr was found to give methyl isobutyrate and formaldehyde (reaction 2)

$$HOCH_2C(CH_3)_2COOCH_3 \rightarrow (CH_3)_2CHCOOCH_3 + CH_2O \quad (2)$$

The theoretical stoichiometry of reaction 2 requires the final pressure, $P_f$, be twice the initial pressure, $P_0$. The average experimental value of $P_f/P_0$ at five different temperatures and ten half-lives is 2.06 (Table 1). Within the experimental error the $P_f/P_0$ confirms the stoichiometry of reaction 2.

Additional verification of the above stoichiometry of reaction 2 was made by comparing, up to 60% decomposition, the pressure measurements and/or the quantitative chromatographic analysis of the substrate with the results of the quantitative chromatographic analysis of the product methyl isobutyrate (Table 2).

The homogeneity of the reaction was checked by using a vessel with a surface-to-volume ratio of 6.0 relative to that of the normal vessel (Table 3). The packed and unpacked clean Pyrex vessel had a small heterogeneous effect on the substrate. However, when the vessels are seasoned with allyl bromide no significant effect on the rate coefficients for elimination of the ester was obtained.

The effect of different proportions of toluene, a free radical inhibitor, had no effect on the rates and no induction period was observed (Table 4). The rate coefficient was reproducible with a relative deviation less than 5% at a given temperature.

The first-order rate coefficient of this hydroxyester calculated from $k_1 = (2.303/t) \log[(2P_0 - P_t)/P_0]$ was independent of the initial pressure (Table 5). A plot of $\log(2P_0 - P_t)$ against time $t$ gave a good straight line up to 60% reaction. The variations of the rate coefficients with temperature are shown in Table 6, where the rate coefficients at the 90% confidence limit obtained by a least-squares procedure and the shown Arrhenius equation are given.

The data presented in Table 7 show that the rate of elimination of methyl 2,2-dimethyl-3-hydroxypropionate is 1.4 greater than that of methyl 3-hydroxypropionate. Apparently, this small but significant difference in rate for the gas phase reaction may result from steric acceleration in the process of decomposition. This argument has suggested carrying out some theoretical calculations on the decomposition of the hydroxyl ester substrate to describe reasonably the elimination mechanism for reaction 2.

## IV. Experimental Method

**Materials.** The substrate methyl 2,2-dimethyl-3-hydroxypropionate, purchased from Aldrich, was distilled until greater than 99.0% purity was obtained [GC/MS (Saturn 2000, Varian) Capillary column DB-5MS, 30 m × 0.250 mm, i.d. 0.25 $\mu$m] was used. Diisodecyl phthalate 5%−Chromosorb G washed with dimethyl chlorosilane 60−80 mesh, 6 ft × 1/8 in., was used as a column for methyl isobutyrate. The verification of the substrate and identifications of the products were carried out by GC/MS (Saturn 2000, Varian) Capillary column DB-5MS, 30 m × 0.250 mm, i.d. 0.25 $\mu$m.

**Kinetics.** The kinetics experiments were performed in a static system as described before.[16−18] The rate coefficients were determined manometrically. The temperature was controlled by a resistance thermometer controller and an Omega Model SSR280A45 solid state relay, maintained within ±0.2 °C and measured with a calibrated platinum−platinum−13% rhodium thermocouple with an Omega DP41-TC/DP41-RTD high performance digital temperature indicator. No temperature gradient was detected along the reaction vessel. The substrate was injected directly into the reaction vessel with a syringe through a silicone rubber septum. The amount of substrates used for each run was ∼0.05−0.1 mL.

## V. Theoretical Results

**Kinetic and Thermodynamic Parameters.** The thermolysis reaction path of 2,2-dimethyl-3-hydroxypropionate to give methyl isobutyrate and formaldehyde was studied at different theory levels. These studies show that the mechanism for decomposition involves a slow step through a six-membered transition state to afford the enol form of methyl isobutyrate and formaldehyde. The former undergoes rapid tautomerization to the keto form. Essentially the same structure for TS was obtained for all theory levels.

The transition state structure was verified using vibrational analysis, by possessing a unique imaginary frequency and also by intrinsic reaction coordinate (IRC) calculations. IRC calculations demonstrated that the TS structure connects the reactant 2,2-dimethyl-3-hydroxypropionate and products methyl isobutyrate (enol form) and formaldehyde in the reaction path. Calculations showed that the reaction path through a six-membered ring is unique to the formation of the above-mentioned products from 2,2-methyl-3-hydroxypropionate.

Calculated kinetic and thermodynamic parameters for the decomposition of methyl 2,2-dimethyl −3-hydroxypropionate to give methyl isobutyrate and formaldehyde are shown in Table 8. Theoretical results for the rate determining step from calculation at different levels of theory for kinetics and thermodynamic parameters, energy of activation, log $A$, enthalpy, entropy, and free energy of activation, showed a better accord to experimental counterparts for DFT methods, particularly the combinations functional/basis set B3LYP/6-211G** level of theory. The use of bigger basis set improved the results, particularly the addition of polarized functions for hydrogen as expected because a hydrogen atom is being transferred in the transition state. DFT functional PBEPBE also gave reasonably good results with the 6-211** basis set. The perturbation method MP2/6-21G renders underestimated reaction barrier. Using factor $C^{exp} = 21.3$, it is possible to better estimate the kinetic and thermodynamic parameters for the elimination of methyl 2,2-dimethy-3-hydroxypropionate in the gas phase.

The negative value for entropy of activation of about −40 kJ/(mol K) implies a considerable loss of degree of freedom in the TS, implying a fairly rigid structure. The study of the enolization step was also carried out. The keto−enol equilibrium favors the keto form and the barrier for this step was found to be $3.52 \times 10^{-2}$ kJ mol$^{-1}$ at B3LYP/6-21G** level. This result confirms that the rate-determining step of the gas phase thermal decomposition of methyl 2,2-dimethyl 3-hydroxypropionate is the formation for formaldehyde and the enol form of methyl isobutyrate.

**Transition State and Mechanism.** The transition vector linked with the imaginary frequency for the TS is associated

**TABLE 2: Stoichiometry of the Reaction**

| substrate | temp (°C) | parameter | value | | | | |
|---|---|---|---|---|---|---|---|
| methyl 2,2-dimethyl-3-hydroxypropionate | 380.5 | time (min) | 3.5 | 5 | 8 | 10 | 15 |
| | | reaction (%) (pressure) | 18.9 | 24.6 | 34.7 | 45.9 | 59.3 |
| | | substrate decomp (%) (GC) | 19.3 | 25.7 | 35.1 | 44.7 | 60.4 |
| | | isobutyrate (%) (GC) | 19.8 | 25.9 | 35.1 | 45.3 | 59.7 |

**TABLE 3: Homogeneity of the Elimination Reaction at 380.5 °C**

| substrate | $S/V$ ($cm^{-1}$)[a] | $10^4k_1$ ($s^{-1}$)[b] | $10^4k_1$ ($s^{-1}$)[c] |
|---|---|---|---|
| methyl 2,2-dimethyl-3-hydroxypropionate | 1 | 10.54 | 9.85 |
| | 6 | 12.07 | 9.82 |

[a] S= surface area; V= volume. [b] Clean Pyrex vessel. [c] Vessel seasoned with allyl bromide.

**TABLE 4: Effect of Free Radical Inhibitor Toluene on Rates at 380.5 °C[a]**

| substrate | $P_s$ (Torr) | $P_i$ (Torr) | $P_i/P_s$ | $10^4k_1$ ($s^{-1}$) |
|---|---|---|---|---|
| methyl 2,2dimethyl-3- hydroxypropionate | 115 | | | 10.01 |
| | 162 | 101 | 0.6 | 9.59 |
| | 92 | 123 | 1.33 | 9.64 |
| | 70 | 130 | 1.86 | 9.88 |
| | 64.5 | 221 | 3.42 | 9.40 |

[a] Seasoned vessel. $P_s$ = pressure substrate. $P_i$ = pressure inhibitor.

**TABLE 5: Invariability of the Rate Coefficients with Initial Pressure**

| substrate | temp (°C) | parameters | value | | | |
|---|---|---|---|---|---|---|
| methyl 2,2-dimethyl-3-hydroxypropionate | 380.5 | $P_0$ (Torr) | 64.5 | 92 | 120 | 162 |
| | | $10^4k_1$ ($s^{-1}$) | 9.40 | 9.64 | 9.55 | 9.59 |

**TABLE 6: Variation of the Rate Coefficients with Temperatures[a]**

| substrate | | value | | | | | | |
|---|---|---|---|---|---|---|---|---|
| methyl 2,2-dimethyl-3-hydroxypropionate | temp (°C) | 349.1 | 359.0 | 369.2 | 380.5 | 390.5 | 399.1 | 410.0 |
| | $10^4k_1$ ($s^{-1}$) | 2.03 | 3.42 | 5.41 | 9.85 | 16.12 | 26.96 | 45.26 |

[a] Rate equation $\log k_1$ ($s^{-1}$) = [(11.43 ± 0.57) − (180.4 ± 7.2) kJ $mol^{-1}$] × $(2.303RT)^{-1}$, $r$ = 0.9990.

**TABLE 7: Comparative Kinetic and Thermodynamic Parameters at 380.0°C**

| substrate | $10^4k_1$ ($s^{-1}$) | $E_a$ (kJ/mol) | $\log A$ ($s^{-1}$) | $\Delta S^{\ddagger}$ [J/(mol K)] | $\Delta H^{\ddagger}$ (kJ/mol) | $\Delta G^{\ddagger}$ (kJ/mol) |
|---|---|---|---|---|---|---|
| methyl 3-hydroxypropionate[a] | 7.30 | 178.1 | 11.11 | − 47.13 | 172.7 | 203.5 |
| methyl 2,2-dimethyl-3-hydroxypropionate | 9.99 | 180.4 ± 7.2 | 11.43 ±0.57 | − 41.01 | 175.0 | 201.8 |

[a] Reference 5.

with the hydrogen transfer from the 3-hydroxy moiety to the oxygen atom at the ester carbonyl in the reactant 2,2-dimethyl-3-hydroxypropionate (Scheme 2, Figure 1) Structural parameters and charges for reactant 2,2-dimethyl-3-hydroxypropionate (R), the transition state (TS), and products methyl isobutyrate and formaldehyde (P) are given in Table 9.

The geometry of the TS is a six-membered ring, involving atoms $C_1$, $C_4$, $O_{13}$, $H_{14}$, $C_{15}$, $O_{16}$, in a semichair like configuration. The hydrogen being transferred ($H_{14}$) is midway between the 3-hydroxyl oxygen ($O_{13}$) and the ester carbonyl oxygen ($O_{16}$) (Scheme 2, Figure 1).

Variation in bond distances, bond angles, and dihedrals can be used to follow the reaction progress from the reactant to the transition state structure to products (Table 9). The $C_4-C_{15}$ bond distance shows the change from a single bond to double bond characteristic of the enol form of methyl isobutyrate. Additionally, the $C_1-O_{13}$ bond distance changes from single to double, as the hydroxyl hydrogen ($H_{14}$) is transferred to form the formaldehyde product. The distance $O_{13}-H_{14}$ goes from 0.97 to ∼1.96 Å, implying bond breaking while the $H_{14}-O_{16}$ distance diminishes from reactant to product as the hydrogen is being transferred. The $C_{15}-O_{16}$ distance increases, owing to the change from double to single bond. The $C_4-C_1$ distance shows the bond breaking from reactant to TS and products. Bond angles (Table 9) show hybridization changes in $C_1$ from $sp^3$ to $sp^2$, $C_4$ and $C_{15}$ from $sp^3$ to $sp^2$, $O_{13}$ from $sp^3$ to $sp^2$, and $O_{16}$ from $sp^2$ to $sp^3$.

NBO analysis was used to study the electron density redistribution in the reaction path as shown in NBO charges from Table 10 from the reactant methyl 2,2-dimethyl-3-hydroxypropionate (R), transition state (TS), and products (P).

There is an increase in electron density at $C_4$ from the reactant to the transition state (−0.19 to −0.25) while $C_1$ becomes positively charged (−0.024 to +0.265). $O_{13}$ show a decrease in electron density (−0.817 to −0.805) and also $H_{14}$ (0.50 to 0.56). Additionally the negative charge in $O_{16}$ increases in the TS (−0.73 to −0.82) while carbon $C_{15}$ decreases in electron density (1.01 to 0.88). These observations suggest that the polarization

**TABLE 8: Calculated Kinetic and Thermodynamic Parameters Obtained for the Elimination Reaction of Methyl 2,2-Dimethyl-3-hydroxypropionate at 380°C and 0.1487 atm**

| methods | $\Delta H^{\ddagger}$ (kJ/mol) | $\Delta S^{\ddagger}$ [J/(mol K)] | $\Delta G^{\ddagger}$ (kJ/mol) | $E_a$ (kJ/mol) | log $A$ | $10^3 k$ ($s^{-1}$) |
|---|---|---|---|---|---|---|
| experimental | 174.97 | −40.93 | 201.7 | 180.40 | 11.43 | 1.00 |
| B3LYP/6-21G* | 208.1 | −29.75 | 227.5 | 213.5 | 12.01 | 8.6 |
| | 204.6 | −40.93 | 231.4 | 210.1 | 11.43 | 4.3 |
| B3LYP/6-21G** | 204.6 | −28.13 | 223.0 | 210.1 | 12.10 | 20.0 |
| | 208.1 | −40.93 | 234.8 | 213.5 | 11.43 | 2.2 |
| B3LYP/6-211G** | 165.0 | 0.68 | 164.1 | 169.94 | 13.60 | 1.03 |
| | 164.9[a] | −40.93 | 191.2 | 169.9 | 11.43 | 6.89 |
| PBEPBE/6-211G** | 160.1 | 12.96 | 151.6 | 165.5 | 14.25 | 10.0 |
| | 160.1 | −40.93 | 186.8 | 165.5 | 11.43 | 15.61 |
| MP2/6-21G | 154.2 | 26.51 | 136.8 | 159.6 | 12.00 | 0.64 |
| | 154.2 | −40.93 | 180.9 | 159.6 | 11.43 | 46.37 |

[a] Calculated using $C^{exp}$ factor.[15]

**SCHEME 2**

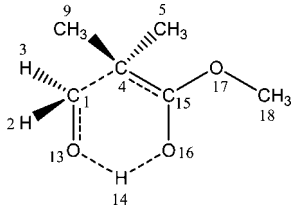


of O13−H14 bond, in the sense $O^{\delta-}\cdots H^{\delta+}$, is determining in the thermal decomposition of methyl 2,2-dimethy-3-hydroxy-lpropionate.

**Bond Order Analysis.** The reaction progress along the reaction pathway was also investigated by means of NBO bond order calculations.[19−21] Wiberg bond indexes[22] were computed using the natural bond orbital NBO program[23] as implemented in Gaussian 03W. These indexes can be used to estimate bond orders from population analysis. Bond breaking and making process involved in the reaction mechanism are monitored by means of the Synchronicity (Sy) concept proposed by Moyano et al.[24] defined by the expression:

$$\mathrm{Sy} = 1 - \left[\sum_{i=1}^{n} \left|\delta B_i - \delta B_{av}\right| / \delta B_{av}\right] / 2n - 2$$

$n$ is the number of bonds directly involved in the reaction and the relative variation of the bond index is obtained from

$$\delta B_i = [B_i^{TS} - B_i^{R}] / [B_i^{P} - B_i^{R}]$$

where the superscripts R, TS, and P represent reactant, transition state, and product, respectively.

The evolution in bond change is calculated as

$$\%\ \mathrm{E}\nu = \delta B_i \times 100$$

The average value is calculated from

$$\delta B_{av} = 1/n \sum_{i=1}^{n} \delta B_i$$

Wiberg bonds indexes $B_i$ are use to follow the changes along the reaction coordinate. The indexes were calculated for those bonds involved in the reaction changes, i.e., $C_4-C_{15}$, $C_{15}-O_{16}$, $C_4-C_1$, $C_1-O_{13}$, $O_{13}-H_{14}$, and $O_{16}-H_{14}$ (Scheme 1, Table 11), all other bond bonds remain practically unaffected during the process.

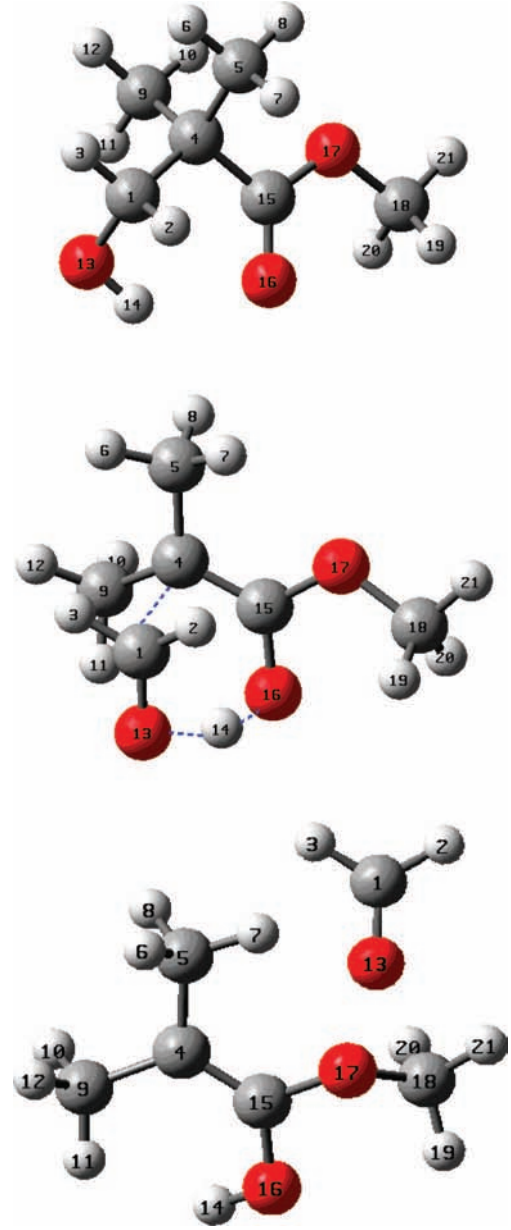

**Figure 1.** Optimized structures for reactant 2,2-dimethyl-3-hydroxypropionate (top), transition state (center), and products methyl isobutyrate and formaldehyde (bottom) at the B3LYP/6-211G(d,p) level of theory. The TS geometry is a semichair six-membered ring.

**TABLE 9: Structural Parameters for Reactant (R), Transition State (TS), and Products for Methyl 2,2-Dimethyl-3-hydroxypropionate Thermal Decomposition from B3LYP/6-311G(d,p) Calculations**

| | Atom Distances (Å) | | | | | |
|---|---|---|---|---|---|---|
| | $C_4-C_{15}$ | $C_{15}-O_{16}$ | $C_4-O_1$ | $C_1-O_{13}$ | $O_{13}-H_{14}$ | $H_{14}-O_{16}$ |
| R | 1.53 | 1.22 | 1.54 | 1.41 | 0.97 | 2.02 |
| TS | 1.35 | 1.36 | 3.11 | 1.21 | 1.88 | 0.98 |
| P | 1.35 | 1.36 | 4.81 | 1.21 | 1.96 | 0.97 |

| | Dihedral Angles (deg) | | | | | |
|---|---|---|---|---|---|---|
| | $C_1-C_4-C_{15}-O_{16}$ | $C_4-C_{15}-O_{16}-H_{14}$ | $C_{15}-O_{16}H_{14}O_{13}$ | $O_{16}-H_{14}O_{13}C_1$ | $H_{14}O_{13}C_1C_4$ | $O_{13}C_1C_4C_{15}$ |
| TS | 68.15 | −49.29 | −5.98 | 0.43 | 31.72 | −61.43 |

| | Imaginary Frequency ($cm^{-1}$) |
|---|---|
| TS | −335.16 |

| | Bond Angles (deg) | | | | | | | |
|---|---|---|---|---|---|---|---|---|
| | $O_{13}C_1C_4$ | $C_1C_4C_{15}$ | $C_4C_{15}O_{16}$ | $C_{15}O_{16}H_{14}$ | $O_{16}H_{14}O_{13}$ | $C_1O_{13}H_{14}$ | $C_3C_1O_{13}$ | $C_9C_4C_5$ |
| R | 114.0 | 108.36 | 125.20 | 100.96 | 131.40 | 104.77 | 106.59 | 110.49 |
| TS | 90.31 | 76.95 | 125.84 | 109.44 | 154.18 | 104.03 | 121.31 | 121.60 |
| P | 55.77 | 58.68 | 127.32 | 111.64 | 142.04 | 103.23 | 121.71 | 122.93 |

**TABLE 10: NBO Charges of the Atoms Involved in the 2,2-Dimethyl-3-hydroxypropionate Thermal Decomposition from B3LYP/6-311G(d,p) Calculations**

| NBO charges | $C_1$ | $C_4$ | $O_{13}$ | $H_{14}$ | $C_{15}$ | $O_{16}$ |
|---|---|---|---|---|---|---|
| reactant | −0.0248 | −0.1906 | −0.8170 | 0.50967 | 1.0157 | −0.7345 |
| transition state | 0.2654 | −0.2597 | −0.8060 | 0.5632 | 0.8844 | −0.8233 |
| products | 0.3413 | −0.2049 | −0.63078 | 0.5329 | 0.7258 | −0.8199 |

**TABLE 11: NBO Analysis for 2,2-Dimethyl-3-hydroxypropionate Thermal Decomposition from B3LYP/6-311G(d,p) Calculations[a]**

| | $C_4-C_{15}$ | $C_{15}-O_{16}$ | $C_4-C_1$ | $C_1-O_{13}$ | $O_{13}-H_{14}$ | $O_{16}-H_{14}$ |
|---|---|---|---|---|---|---|
| $B_i^R$ | 0.961 | 1.669 | 0.974 | 0.931 | 0.713 | 0.015 |
| $B_i^{ET}$ | 1.472 | 1.076 | 0.293 | 1.446 | 0.128 | 0.532 |
| $B_i^P$ | 1.785 | 0.958 | 0.0002 | 1.819 | 0.024 | 0.675 |
| % Ev | 61.98 | 83.3 | 69.95 | 57.94 | 84.94 | 21.64 |
| | | $\delta B_{Prom} = 0.633$ | | | Sy = 0.847 | |

[a] Wiberg bond indexes ($B_i$), % evolution through the reaction coordinate (% Ev), are shown for reactants R, TS-I and products P. Average bond index variation ($\delta B_{av}$) and synchronicity parameter (Sy) are also reported.

Analysis of Wiberg bond indexes reveals more progress in the breaking of $O_{13}-H_{14}$ (84.94%), implying a strong polarization of this bond in the transition state, as well as an important progress in the bond order change for $C_{15}-O_{16}$ (83.3%). The formation of $O_{16}-H_{14}$ is at an early stage in the transition state (21.64%). The reaction progress is intermediate for the other reaction coordinates, showing a progress between 57 and 69%. The decomposition process is dominated by the hydrogen transfer from the hydroxyl oxygen $O_{13}$ to the carbonyl oxygen $O_{16}$ of the ester moiety. The synchronicity parameter Sy = 0.8247 suggests a polarized, moderately asynchronic process, with a late TS in the sense of the hydrogen transfer from the hydroxyl moiety and double bond formation $C_{15}-O_{16}$ and an early TS in the $O_{16}-H_{14}$ bond formation reaction coordinate. The above-mentioned considerations seem to provide evidence for a concerted mechanism, occurring through a moderately polar TS, for the gas phase thermal decomposition of methyl 2,2-dimethyl-3-hydroxypropionate.

## VII. Conclusions

The gas phase elimination of methyl 2,2-dimethyl-3-hydroxypropionate into methyl isobutyrate and formaldehyde was found to be homogeneous and unimolecular and to follow a first-order kinetics. The reaction path was studied by means of electronic structure calculations at different theory levels. The DFT methods of B3LYP/6-211G(d,p) and PBEPBE/6-211G(d,p) produced kinetic and thermodynamic parameters in reasonably better accord with experimental counterparts than MP2 methods. The reaction proceeds through a six-membered ring TS structure in semichair configuration. Theoretical calculations suggest that the reaction proceeds through a concerted polar moderately asynchronous mechanism. NBO charges analysis and bond order suggest that the polarization of hydroxyl $O_{13}-H_{14}$ bond, in the sense $O^{\delta-}\cdots H^{\delta+}$, is determining in the thermal decomposition of methyl 2,2-dimethy-3-hydroxylpropionate and dominates the decomposition process. The transition vector and Wiberg bond indexes imply that the reaction is governed by the hydrogen transfer from the OH group to the oxygen at the ester carbonyl ($O_{16}$) and the $C_{15}-O_{16}$ bond order change.

**Acknowledgment.** T.C. is grateful to the Consejo de Desarrollo Científico y Humanístico (CDCH) for Grant No. PG-03-00-6499-2006.

## References and Notes

(1) Yates, B. L.; Quijano, J. *J. Org. Chem.* **1970**, *35*, 1239–1240.

(2) Yates, B. L.; Ramirez, A.; Velasquez, O. *J. Org. Chem.* **1971**, *36*, 3579–3582.

(3) Taylor, R. In *Acid Derivatives*; Patai, Saul, Ed.; The Chemistry of Functional Group. Suplementary Volume B; Wiley: London, 1979; Chapter 15, pp 859−914.

(4) Holbrook, K. A. In *Vapor and Gas phase Reaction of Carboxylic Acids and their Derivatives*; Patai, Saul, Ed.; The Chemistry of Acid Derivatives.Volume 2; Wiley: London, 1992; Chapter 12, pp 703−746.

(5) August, R.; McEwen, I.; Taylor, R. *J. Chem Soc., Perkin Trans. 2* **1987**, 1683–1689.

(6) Kao, J. J. *Mol. Structure (THEOCHEM).* **1988**, *180*, 383–387.

(7) Sanchez, C.; Quijano, J.; Notario, R. *J. Phys. Org. Chem.* **2004**, *17*, 294–302.

(8) O'Neal, H. E.; Benson, S. W. *J. Phys. Chem.* **1967**, *71*, 29032921;Benson, S. W. *Thermochemical Kinetics*; John Wiley & Sons: New York, 1968.

(9) Zapata, E.; Gaviria, J.; Quijano, J *Int. J. Chem. Kinet* **2007**, *39*, 92–96.

(10) Houminer, Y.; Kao, J.; Seeman, J. I. *J. Chem. Soc., Chem. Commun.* **1984**, 1608–1609.

(11) Frisch, M. J.; Trucks, G. W.; Schlegel, H. B.; Scuseria, G. E.; Robb, M. A.; Cheeseman, J. R.; Montgomery, J. A., Jr.; Vreven, T.; Kudin, K. N.; Burant, J. C.; Millam, J. M.; Iyengar, S. S.; Tomasi, J.; Barone, V.; Mennucci, B.; Cossi, M.; Scalmani, G.; Rega, N.; Petersson, G. A.; Nakatsuji, H.; Hada, M.; Ehara, M.; Toyota, K.; Fukuda, R.; Hasegawa, J.; Ishida, M.; Nakajima, T.; Honda, Y.; Kitao, O.; Nakai, H.; Klene, M.; Li, X.; Knox, J. E.; Hratchian, H. P.; Cross, J. B.; Bakken, V.; Adamo, C.; Jaramillo, J.; Gomperts, R.; Stratmann, R. E.; Yazyev, O; Austin, A. J.; Cammi, R.; Pomelli, C.; Ochterski, J. W.; Ayala, P. Y.; Morokuma, K.; Voth; G. A.; Salvador, P.; Dannenberg, J. J.; Zakrzewski, V. G.; Dapprich, S.; Daniels, A. D.; Strain, M. C.; Farkas, O.; Malick, D. K.; Rabuck, A. D.; Raghavachari, K.; Foresman, J. B.; Ortiz, J. V; Cui, Q.; Baboul, A. G.; Clifford, S.; Cioslowski, J.; Stefanov, B. B.; Liu, G.; Liashenko, A.; Piskorz, P.; Komaromi, I.; Martin, R. L.; Fox, D. J.; Keith, T.; Al-Laham, M. A.; Peng, C. Y.; Nanayakkara, A.; Challacombe, M.; Gill, P. M. W.; Johnson, B.; Chen, W.; Wong, M. W.; Gonzalez, C.; Pople, J. A. *Gaussian 03*, revision C.02; Gaussian, Inc.: Wallingford, CT, 2004.

(12) McQuarrie, D. *Statistical Mechanics*, Harper & Row: New York, 1986.

(13) Foresman, J. B.; Frish, A. E. *Exploring Chemistry with Electronic Methods*, 2nd ed.; Gaussian, Inc.: Pittsburgh, PA, 1996.

(14) Benson, S. W. *The Foundations of Chemical Kinetics*; Mc-Graw-Hill: New York, 1960.

(15) Rotinov, A; Dominguez, R. M.; Cordova, T.; Chuchani, G. *J. Phys. Org. Chem,* **2005**, *18*, 616–624.

(16) Maccoll, A. *J. Chem. Soc.* **1955**, 965–973.

(17) Swinbourne, E. S. *Aust. J. Chem.* **1958**, *11*, 314–330.

(18) Dominguez, R. M; Herize, A; Rotinov, A.; Alvarez-Aular, A.; Visbal, G.; Chuchani, G. *J. Phys. Org. Chem.* **2004**, *17*, 399–408.

(19) Lendvay, G. L. *J. Phys. Chem.* **1989**, *93*, 4422–4429.

(20) Reed, A. E.; Weinstock, R. B.; Weinhold, F. *J. Chem. Phys.* **1985**, *83* (2), 735–746.

(21) Reed, A. E.; Curtiss, L. A.; Weinhold, F. *Chem. Rev.* **1988**, *88*, 899–926.

(22) Wiberg, K. W. *Tetrahedron* **1968**, *24*, 1083–1095.

(23) Reed, A. E.; Carpenter, J. E.; Weinhold, F. NBO, version 3.1.

(24) Moyano, A.; Periclas, M. A.; Valenti, E. *J. Org. Chem.* **1989**, *54*, 573–582.

JP810649W